Detailed discussion of a linear electric field frequency shift (important for next generation) electric dipole moment searches) induced in confined gases by a magnetic field gradient: Implications for electric dipole moment experiments (II)

A.L. Barabanov#, R. Golub+ and SK Lamoreaux*
#Kurchatov Institute
123182 Moscow, Russia
+Physics Department
North Carolina State University
Raleigh, NC 27606
*University of California,
Los Alamos National Laboratory
Physics Division
Los Alamos NM 87545

November 29, 2005

Abstract

The search for particle electric dipole moments represents a most promising way to search for physics beyond the standard model. A number of groups are planning a new generation of experiments using stored gases of various kinds. In order to achieve the target sensitivities it will be necessary to deal with the systematic error resulting from the interaction of the well-known $\vec{v} \times \vec{E}$ field with magnetic field gradients (often referred to as the geometric phase effect [9], [10]. This interaction produces a frequency shift linear in the electric field, mimicking an edm. In this work we introduce an analytic model for the correlation function which determines the behavior of the frequency shift [11] and show in detail how it depends on the operating conditions of the experiment. We also propose a method to directly measure ths correlation function under the exact conditions of a given experiment.

Contents

1 Introduction

The proposition that the search for particle electric dipole moments (edm) represents a reasonable method to look for physics beyond the standard model [1] is inspiring many groups to search for edm's in a variety of systems. (See [2] for a recent review). Experiments on several systems including the neutron [3], and several species of confined gases [4] including Radium [5], Radon [6] and Xenon [7] are in various stages of preparation. These experiments are all hoping to reach sensitivities in the range of $10^{-27} - 10^{-28} e - cm$. Sensitivity in this range has already been achieved in the case of Hg [8]. The experiments proposed represent a broad range of operating conditions, from room temperature gases with buffer gas to laser cooled atoms in a MOT.

In order to achieve the target sensitivities it will be necessary to deal with the systematic error resulting from the interaction of the well-known $\vec{v} \times \vec{E}$ field with magnetic field gradients. Often referred to as the geometric phase effect [9], [10] this interaction produces a frequency shift linear in the electric field, mimicking an edm. This systematic effect is highly dependent on the operating conditions of the experiment. While experiments in small vessels and with high pressure buffer gas are expected to be relatively insensitive to the systematic effect, each of the proposed experiments will have to be analyzed in detail to judge its sensitivity to the effect and to find methods of dealing with it. In this work we introduce an analytic form of the correlation function which determines the behavior of the frequency shift [11] and show in detail how it depends on the operating conditions of the experiment. For clarity we specialize the discussion to to the Los Alamos proposal for a neutron edm search using Ultra-cold neutrons (UCN) and He^3 atoms diffusing in superfluid He^4 as a co-magnetometer, [12] but the generalization to other cases is straightforward.

First analyzed by Commins [9] in the context of a beam experiment, the frequency shift has been discussed in some detail by Pendlebury et al [10] in connection with experiments involving stored particle gases. Additional discussion and calculations have been given by [11].

Our present understanding of the effect can best be summarized by figure 1, which appeared as figure 3 in [11]. This is a plot of the normalized (linear in E) frequency shift vs. normalized Larmor frequency for various values of collision mean free path and wall specularity.

These results have been obtained by numerical simulation of the position-velocity correlation function and taking the Fourier transform. According to [[11], equ 26] the frequency shift is given by

$$\delta\omega = ab \lim_{t\to\infty} \int_0^t d\tau R(\tau) \cos\omega_o \tau \tag{1}$$

where $R(\tau)$ is the position velocity correlation function defined in [[11], equ. 27]:

$$R(\tau) = \langle \overrightarrow{r}(t) \cdot \overrightarrow{v}(t-\tau) - \overrightarrow{r}(t-\tau) \cdot \overrightarrow{v}(t) \rangle \tag{2}$$

and $a = \frac{\gamma}{2} \partial B_z / \partial z$, $b = \gamma E/c$. From the experimental point of view it is very appealing to try to make use of the zero crossing, apparent in figure 1, to reduce the effect.

In this note we present an analytic model for the correlation function $R(\tau)$ and compare it to the results obtained previously by numerical simulations. Using the limiting form of this model, valid for collision mean free paths small compared to the vessel size, we calculate the temperature dependence of the frequency shift for ^3He diffusing in superfluid ^4He. This is an experimentally favored regime as collisions are seen to reduce the effect, as well as the slope at the zero crossing, considerably. We also propose a method for measuring the spectrum of the correlation function, *i.e.* the frequency dependence of the shift, directly.

2 Analytical model for the correlation function $R(\tau)$

2.1 Gas collisions

1) We consider a particle that moves among scattering centers. If τ_c is the average time between collisions the velocity autocorrelation function will have

the form [14]

$$\psi(t) \equiv \langle \vec{v}(t)\vec{v}(0)\rangle = v^2\, e^{-\frac{\tau}{\tau_c}}. \tag{3}$$

In the other words, $\psi(t)$ obeys the equation:

$$\frac{d\psi(t)}{dt} + \frac{1}{\tau_c}\psi(t) = 0. \tag{4}$$

2.2 Wall collisions

We consider particles moving in a cylindrical storage cell in a vacuum. As shown in [10],[11] the frequency shift depends only on the motion in the x, y plane. Referring to figure 2, the trajectory sweeps out an angle

$$\alpha = \arccos{(r/R)}$$

with respect to the center in a time

$$\frac{\tau_{wall}}{2} = \frac{\sqrt{R^2 - r^2}}{v}$$

where τ_{wall} is the time between wall collisions. The average angular velocity for a single trajectory is then

$$\omega = \frac{\arccos{(r/R)}\, v}{\sqrt{R^2 - r^2}}.$$

The average squared frequency for all particles with velocity v (in the x, y plane) has been given by [10], equ, (28) as

$$\langle \omega_o^2 \rangle = \frac{\pi^2}{6}\left(\frac{v^2}{R^2}\right) \tag{5}$$

As the motion is not strictly circular each trajectory will experience a complicated spectrum for the time varying field (Ref. [10], section IV D and figure 7), but the mean square of the fundamental frequency will be given by (5).

Assuming that the result is dominated by the fundamental frequency, the velocity autocorrelation function will, to this approximation , obey the equation:

$$\frac{d^2\psi(t)}{dt^2} + \langle \omega_o^2 \rangle\, \psi(t) = 0, \tag{6}$$

2.2.1 Non-specular wall collisions

Following the proceeding section we are modelling the correlation function as a harmonic oscillator. During one traversal of the cell the oscillator will undergo a phase change

$$\phi = \omega\tau_{wall} = 2\alpha = 2\arccos{(r/R)}$$

A non-specular reflection from the wall would result in a change in the incident angle for the next collision, χ, by a random amount $\Delta\chi$ and hence a change in the accumulated oscillator phase by

$$\begin{aligned}\Delta\phi &= \frac{d\phi}{d\chi}\Delta\chi \\ \frac{d\phi}{d\chi} &= \frac{d\phi}{dr}\frac{dr}{d\chi}\end{aligned}$$

With

$$\begin{aligned}\sin\chi &= r/R \\ \cos\chi &= \sqrt{1 - r^2/R^2}\end{aligned}$$

we have

$$\begin{aligned}\frac{d\chi}{dr} &= \frac{1}{\sqrt{R^2 - r^2}} \\ \frac{d\phi}{dr} &= \frac{2}{R\sqrt{1 - r^2/R^2}}\end{aligned}$$

so

$$\Delta\phi = 2\Delta\chi$$

Since the changes $\Delta\phi$ are random the phase ϕ will make a random walk so that after a time t we will have

$$\left\langle (\Delta\phi)^2 \right\rangle_t = 4\left\langle (\Delta\chi)^2 \right\rangle \frac{t}{\tau_{wall}} = 2\left\langle (\Delta\chi)^2 \right\rangle \frac{tv}{\sqrt{R^2 - r^2}}$$

Averaging the amplitude of the oscillator over the distribution of $\Delta\phi$ the amplitude will be reduced by

$$\langle \cos\phi \rangle = 1 - \frac{1}{2}\left\langle (\Delta\phi)^2 \right\rangle_t \equiv 1 - \frac{t}{\tau_{non-spec}} \sim \exp\left(-\frac{t}{\tau_{non-spec}}\right)$$

Thus we have

$$\frac{1}{\tau_{non-spec}} = \frac{\left\langle (\Delta\chi)^2 \right\rangle v}{\sqrt{R^2 - r^2}}.$$

Averaging over r we find

$$\left\langle \frac{1}{\tau_{non-spec}} \right\rangle = \left\langle (\Delta\chi)^2 \right\rangle v \int_0^R \frac{F(r)\,dr}{\sqrt{R^2 - r^2}} = \frac{4}{\pi}\left\langle (\Delta\chi)^2 \right\rangle \frac{v}{R},$$

where $F(r)\,dr$ is the probability that a trajectory has a pericentric distance between $r, r + dr$:

$$F(r) = \frac{4\sqrt{R^2 - r^2}}{\pi R^2}.$$

2.3 Model expression for the correlation function

When the particles are moving inside a vessel containing scatterers, one can expect that the equation for the velocity correlation function is the combination of (4) and (6), thus we are led to write

$$\frac{d^2\psi(\tau)}{d\tau^2} + \frac{1}{\tau_c}\frac{d\psi(\tau)}{d\tau} + \left\langle \omega_0^2 \right\rangle \psi(\tau) = 0. \tag{7}$$

This is just the equation for a damped harmonic oscillator and its general solution is of the form:

$$\psi(\tau) = c_1 e^{-\eta_1 \tau} + c_2 e^{-\eta_2 \tau}, \tag{8}$$

where

$$\eta_1 = \frac{1}{2\tau_c} + \sqrt{\frac{1}{4\tau_c^2} - \langle \omega_0^2 \rangle}, \qquad \eta_2 = \frac{1}{2\tau_c} - \sqrt{\frac{1}{4\tau_c^2} - \langle \omega_0^2 \rangle}. \tag{9}$$

Then, we have for the boundary condition satisfied by $\psi(\tau)$, [11]

$$h(\tau) = \int_0^\tau \psi(t)dt = \frac{R(\tau)}{2} \to 0, \qquad \text{when} \qquad \tau \to \infty.$$

Thus, the velocity correlation function $[\psi(\tau) = \langle \vec{v}(t)\vec{v}(0) \rangle]$ will have the form:

$$\psi(\tau) = \frac{\eta_1 v^2}{\eta_1 - \eta_2}\left(e^{-\eta_1 \tau} - \frac{\eta_2}{\eta_1} e^{-\eta_2 \tau} \right). \tag{10}$$

and the function $R(\tau)$ will be given by:

$$R(\tau) = 2\int_0^\tau \psi(x)dx = \frac{2v^2}{\eta_1 - \eta_2}\left(1 - e^{-(\eta_1 - \eta_2)\tau}\right) e^{-\eta_2 \tau}. \tag{11}$$

2.3.1 Overdamped, short mean free path, limit

In the overdamped limit

$$\frac{1}{2\tau_c} \gg \omega_0 \tag{12}$$

we find:

$$\eta_1 \simeq \frac{1}{\tau_c}, \qquad \eta_2 \simeq \tau_c \left\langle \omega_0^2 \right\rangle, \qquad \eta_1 \gg \eta_2. \tag{13}$$

Therefore:

$$R(\tau) = 2\lambda v \left(1 - e^{-\frac{\tau}{\tau_c}}\right) e^{-\frac{\tau}{T}}, \tag{14}$$

with

$$T = \frac{1}{\tau_c \langle \omega_0^2 \rangle} = \left(\frac{6}{\pi^2}\right)\frac{R^2}{v\lambda}. \tag{15}$$

using (5).

The numerical simulations of the correlation function shown in figure 1 of [11] (for a cylinder), were seen to be in good agreement (in the short mean free path limit) with equ. (14) above (equation 43, [11]) with

$$T = .6R^2/\lambda v \tag{16}$$

where λ is the collision mean free path, v is the particle velocity and R is the radius of the cylindrical measurement cell, (taken as $R = 25$, in the rest of this paper). The factor 0.6 in equation (16) is in good agreement with the factor $\left(6/\pi^2 = 0.608\right)$ in equation (15).

In the case of He^3 moving in superfluid He^4, τ_c, v and λ are all functions of temperature For UCN on the other hand the only collisions are those with the walls, all parameters are independent of temperature and we have to take the limit

$$\frac{1}{2\tau_c} \ll \omega_0.$$

In figure 3 we show a comparison of the correlation functions calculated by numerical simulation, red, the model equ. (11), blue and the short mean free path limit (14), green.

In the figures $r_o = R/\lambda$. We see the model gives a reasonable fit for a wide range of r_o and the short mean free path expression (14), (green), is a reasonable fit for $r_o \gtrsim 2.5$. The disagreement for smaller r_o is most likely due to the neglect in our model of higher harmonics of the motional frequency

In the following we will use (14) to calculate the frequency shift averaged over a Maxwell-Boltzman velocity distribution as a function of temperature for ${}^3He$ diffusing in ${}^4He$, taking into account the velocity dependence of the mean free path.

2.4 Calculation of the zero crossing frequency for the $\mathbf{v}\times E$ induced systematic

According to (1) the frequency shift is proportional to $S(\omega)$, the cosine Fourier transform of $R(\tau)$ which is given by (2). For $\exp(-\alpha|\tau|)$ the cosine Fourier transform is $\alpha/\left(\alpha^2+\omega^2\right)$ so that we have, using the short mean free path limit of the model, equation (14)

$$S(\omega) = \left[\frac{\eta_2}{\omega^2+\eta_2^2} - \frac{\eta_1+\eta_2}{\omega^2+(\eta_1+\eta_2)^2}\right]\lambda v \tag{17}$$

This is easily seen to have the correct limits for $\omega \to 0, \infty$, (equations 54 and 70 in [11]). To find the value of ω where the effect goes to zero we put

$$S(\omega) = 0$$

$$\omega^2 + (\eta_1+\eta_2)^2 = \left(\omega^2+\eta_2^2\right)\frac{(\eta_1+\eta_2)}{\eta_2}$$

$$\omega = \sqrt{\eta_1\eta_2+\eta_2^2} \approx \sqrt{\eta_1\eta_2}$$

in the case where $\eta_1 \gg \eta_2 \quad (\lambda \ll R)$. Thus we see that the zero crossing, in the limit, is at

$$\omega_o \approx \sqrt{\eta_1 \eta_2} = \sqrt{\frac{\lambda v}{.6R^2 \tau_c}} = 1.3 \frac{v}{R}$$

which should hold for reasonably small values of λ/R. Thus for short λ all curves should have the same zero crossing. This is seen to be satisfied by the numerical simulations of figure 1.

3 Frequency shift averaged over velocity distribution

Using the limiting analytical model (14) for the correlation function and its Fourier transform we can perform an average over the velocity distribution. We do this for the case (1) of a constant collision man free path and then for the realistic case (2) of a mean free path proportional to velocity in order to show the influence of a variable collision mean free path.

3.1 Mean free path independent of velocity

The frequency shift, is given in terms of the spectrum $S(\omega)$ (17) by:

$$\delta\omega(\omega, T) = abS(\omega)$$

$$\delta\omega(\omega, T) = abR^2 \, (.6) \left[\frac{(k(T)/.6)^2}{(\omega R/v)^2 + (k(T)/.6)^2} - \frac{(k(T)/.6)\,(k(T)/.6 + 1/k(T))}{(\omega R/v)^2 + (k(T)/.6 + 1/k(T))^2} \right] \tag{18}$$

with $k = \lambda/R = 1/r_o$ being a function of temperature ($\lambda(T) = 3D(T)/v(T)$) as shown in figure 3c), ($D(T) = 1.6/T^7$ is the diffusion coefficient for He^3 in He^4 as measured by [13], and we have taken $R = 25$) .

The average of this over the velocity distribution of the He^3 will be given by

$$\begin{aligned} \langle \delta\omega(\omega, T) \rangle &= \frac{4}{\sqrt{\pi}} \int \delta\omega(\omega, T) \frac{v^2}{\beta^2} e^{-v^2/\beta^2} \frac{dv}{\beta} \\ &= abR^2 \, (.6) \frac{4}{\sqrt{\pi}} \int_0^\infty \left[\frac{1}{(\omega R/\alpha_2)^2 + v^2} - \frac{\alpha_2/\alpha_1}{(\omega R/\alpha_1)^2 + v^2} \right] v^4 e^{-v^2/\beta^2} \frac{dv}{\beta^3} \end{aligned}$$

where $\alpha_2 = (k(T)/.6)$, $\alpha_1 = (k(T)/.6 + 1/k(T))$. Now we have

$$\frac{4}{\sqrt{\pi}} \int_0^\infty \frac{x^4}{a^2 + x^2} e^{-x^2/\beta^2} dx \equiv F(a, \beta) = 2a^3 \sqrt{\pi} e^{\frac{a^2}{\beta^2}} \left(1 - \text{erf}\left(\frac{a}{\beta}\right) \right) - 2a^2\beta + \beta^3 \tag{19}$$

so that

$$\begin{aligned}\langle \delta\omega(\omega,T)\rangle &= \frac{abR^2}{\beta^3}(.6)\left[F\left(\frac{\omega R}{\alpha_2},\beta(T)\right)-\frac{\alpha_2}{\alpha_1}F\left(\frac{\omega R}{\alpha_1},\beta(T)\right)\right]\\ &\equiv abR^2\Omega(\omega,T)\end{aligned}$$

where $\beta(T)=1.28\times10^4\sqrt{\frac{T}{7.2}}cm/\sec$ is the most probable velocity for He^3 in He^4. $F(a,\beta)$ tends to be difficult to calculate numerically for $\alpha/\beta \gtrsim 5$ so we will use the asymptotic expansion (Ref. [15], section 7.1.23, pg 298)

$$\sqrt{\pi}e^{z^2}\operatorname{erf}c(z)\to\left(\frac{1}{z}\right)\left(1-\frac{1}{2z^2}+\frac{3}{4z^4}-\frac{15}{8z^6}+....\right)$$

for $\alpha/\beta>4$. Note that the leading term in the expansion is canceled by the term $2a^2\beta$ in (19). To plot the results we choose

$$X(\omega,T)=\omega R/\beta(T) \tag{20}$$

as the independent variable.

Figure 4 shows the normalized, averaged over the velocity distribution, frequency shift plotted versus the frequency relative to the appropriate, most probable velocity, (20):

Expanding the plot we see the region near the zero crossing (figure 5).
and expanding still further (figure 6)

In this figure we see the zero crossings converging as the mean free path gets smaller (increasing temperature) just as in the single velocity case (section 2.4).

From the point of view of an experiment it is perhaps more interesting to plot the results as a function of temperature.

Figure 7 shows the temperature dependence of the velocity averaged frequency shift for a range of frequencies specified by the corresponding values of $X(\omega,T)$, (equ. 20), i.e. $\omega=\frac{\beta(T)}{R}X(\omega,T)$.

Expanding the plot (figure 8) shows the region where the effect can be minimized:

Here we see that the applied frequency can be chosen so that the velocity averaging does indeed reduce the effect. In fact reductions of 10^{-5} to 10^{-6} appear feasible.

3.2 Mean free path $\propto velocity$, cross section $\sim 1/v$

We have $k(T)=\lambda(T)/R$. Since the velocity of the He^3 is much less than the phonon velocity ($2.2\times10^4 cm/\sec$) the collision rate of phonons with the He^3 will be independent of the He^3 velocity. In a time τ_c a He^3 with velocity v, will move a distance $\lambda_v(T)=v\tau_c(T)$. Thus

$$k_v(T)=\lambda_v(T)/R=v\tau_c(T)/R=v/s(T)$$

with $s(T) = R/\tau_c(T)$.

From equation (18)

$$\delta\omega(\omega,T) = abR^2\,(.6)\left[\frac{\left(k_v(T)/.6\right)^2}{\left(\omega R/v\right)^2 + \left(k_v(T)/.6\right)^2} - \frac{\left(k_v(T)/.6\right)\left(k_v(T)/.6 + 1/k_v(T)\right)}{\left(\omega R/v\right)^2 + \left(k_v(T)/.6 + 1/k_v(T)\right)^2}\right] \tag{21}$$

The average of this over the velocity distribution of the He^3 will be given by

$$\langle\delta\omega(\omega,T)\rangle = \frac{4}{\sqrt{\pi}}\int \delta\omega(\omega,T)\frac{v^2}{\beta^2}e^{-v^2/\beta^2}\frac{dv}{\beta}$$

$$= abR^2\,(.6)\,\frac{4}{\sqrt{\pi}}\int_0^\infty \left[\frac{1}{\left(\omega R/\alpha_2\right)^2 + v^2} - \frac{\alpha_2/\alpha_1}{\left(\omega R/\alpha_1\right)^2 + v^2}\right] v^4 e^{-v^2/\beta^2}\frac{dv}{\beta^3} \tag{22}$$

$$\equiv abR^2\Psi\,(\omega,T) \tag{23}$$

where $\alpha_2 = \left(k_v(T)/.6\right)$, $\alpha_1 = \left(k_v(T)/.6 + 1/k_v(T)\right)$. In the region of interest for suppression of the effect, $k_v(T) \ll 1$, we have $\alpha_1 \sim 1/k_v(T)$. Then the integral in (22) can be written

$$= \int_0^\infty \left[\frac{y^2}{\left(\frac{.6s}{\beta(T)}\right)^2\left(\frac{\omega R}{\beta(T)}\right)^2 + y^4} - \frac{1/.6}{\left(\frac{\omega R}{\beta(T)}\right)^2 + \frac{s(T)^2}{\beta(T)^2}}\right] y^4 e^{-y^2}dy$$

where $y = v/\beta(T)$. The second integral can be evaluated as

$$\int_0^\infty y^4 e^{-y^2}dy = \frac{3}{2}\frac{\sqrt{\pi}}{4}$$

Defining

$$x(\omega,T) = \frac{\omega R}{\beta(T)}$$

and writing

$$\frac{s(T)}{\beta(T)} = \frac{R}{\beta(T)\tau_c(T)} = \frac{R}{\lambda_c(T)} = \frac{1}{k(T)}$$

where $\lambda_c(T)$ and $k(T)$ are evaluated at the most probable velocity $\beta(T)$, we have $a(T) = \left(\frac{.6s}{\beta(T)}\right)\left(\frac{\omega R}{\beta(T)}\right) = \frac{.6}{k(T)}x(\omega,T)$

The first integral can be evaluated in terms of a hypergeometric function (hypergeom $\left([1], \left[\frac{1}{4}, -\frac{1}{4}\right], -\frac{1}{4}x^2\right)$) but the series for this has some convergence difficulties for the parameters of interest. Thus we define

$$f(a) = \int_0^\infty \frac{y^6}{a^2 + y^4}e^{-y^2}dy$$

(to be evaluated numerically as the integrand is well behaved) so that

$$\Psi\left(\omega,T\right)=(.6)\left[\frac{4}{\sqrt{\pi}}f\left[\frac{.6}{k(T)}x(\omega,T)\right]-\frac{2.5}{\left(x(\omega,T)\right)^{2}+\left(\frac{1}{k(T)}\right)^{2}}\right] \tag{24}$$

In figure 9 we plot the frequency shift averaged over velocity as a function of Larmor frequency for fixed temperature taking into account the velocity dependence of the mean free path.

Figures 10 and 11 show the frequency shift as a function of temperature for various frequencies

4 Measurement of the correlation function, $R\left(\tau\right)$

While the theory presented here is expected to be accurate for the case of polarized He^3 diffusing in superfluid He^4 it would be nice to be able to confirm it experimentally and to check its applicability to other edm searches in progress. In this section we present a generally applicable, straightforward method to measure the frequency spectrum of the relevant correlation function (2) and hence the frequency dependence of the frequency shift directly.

If we apply a uniform magnetic field gradient $\partial B_z/\partial z$ large enough so that it dominates all other field gradients that may be present, there will be a radial field in the $x-y$ plane $\overrightarrow{B}_{\overrightarrow{r}}=-\left(\overrightarrow{r}/2\right)\left(\partial B_z/\partial z\right)$. Then

$$\frac{\partial B_{x,y}}{\partial x,y}=-\frac{1}{2}\frac{\partial B_z}{\partial z}=-a$$

and the field correlation functions will be

$$\left\langle B_{x_i}\left(t\right)B_{x_i}\left(t+\tau\right)\right\rangle=\left(a\right)^2\left\langle x_i\left(t\right)x_i\left(t+\tau\right)\right\rangle$$

where $x_i=x$ or y. Then following McGregor [14] the relaxation time, T_1 will be given by (in the case when $\partial B_z/\partial z$ is large enough so that wall relaxation can be neglected)

$$\frac{1}{T_1}=\frac{\gamma^2a^2}{2}\left[S_r\left(\omega_o\right)\right]$$

with

$$\begin{aligned}S_r\left(\omega\right)&=\int_{-\infty}^{\infty}\left\langle\overrightarrow{r_\perp}\left(t\right)\cdot\overrightarrow{r_\perp}\left(t+\tau\right)\right\rangle e^{-i\omega\tau}d\tau\\&=\int_{-\infty}^{\infty}R_{\overrightarrow{r}\overrightarrow{r}}\left(\tau\right)\cos\omega\tau d\tau\end{aligned}$$

where we recognize that the correlation function $R_{\vec{r}\vec{r}}(\tau)$ is an even function of τ. A measurement of T_1 will thus yield the function $S_r(\omega)$. Now

$$\begin{aligned}\omega^2 S_r(\omega) &= -\int_{-\infty}^{\infty} R_{\vec{r}\vec{r}}(\tau)\frac{d^2}{d\tau^2}(\cos\omega\tau)\,d\tau \\ &= -\int_{-\infty}^{\infty} \frac{d^2 R_{\vec{r}\vec{r}}(\tau)}{d\tau^2}(\cos\omega\tau)\,d\tau \\ &= \int_{-\infty}^{\infty} R_{\vec{v}\vec{v}}(\tau)(\cos\omega\tau)\,d\tau\end{aligned}$$

where we used $R_{\vec{v}\vec{v}}(\tau) = -d^2R_{\vec{r}\vec{r}}(\tau)/d\tau^2$ [16] for the velocity correlation function. Then

$$R_{\vec{v}\vec{v}}(\tau) = \frac{1}{2\pi}\int_{-\infty}^{\infty} \omega^2 S_r(\omega)\cos\omega\tau d\tau$$

By comparison with equ (38) of [11] we identify $\omega^2 S_r(\omega)/2\pi$ with $\psi(\omega)$ of that work and we then see that the systematic frequency shift is given by (equation 40 of [11])

$$\delta\omega = -\frac{ab}{2\pi}\int_{-\infty}^{\infty}\frac{\omega^2 S_r(\omega)}{(\omega_o^2-\omega^2)}d\omega \tag{25}$$

Since we can determine $S_r(\omega)$ from the T_1 measurements we can determine the frequency dependence of the systematic frequency shift for any experimental conditions without the need of applying an electric field.

5 Arbitrary Magnetic field geometry

Our discussion has assumed a magnetic field configuration with $G_z = \partial B_z/\partial z$ constant. Pendlebury et al [10] have shown, using a geometric phase argument, that regardless of the field geometry the effect only depends on the volume average of G_z in the high frequency (called by them the adiabatic) limit. In a recent note, Harris and Pendlebury [17] have shown that in the case of a field produced by a dipole external to the measurement cell, this does not hold in the low frequency (diffusion) limit. In this section we discuss this problem using our correlation function approach in order to give some physical insight into what is happening and display details of the transition from one case to another.

5.1 Short time (high frequency, adiabatic) limit of the correlation function

Reference [11], has shown that the systematic edm is given, in general, as the Fourier transform of a certain correlation function of the time varying field seen by the neutrons as they move through the apparatus. Equation (23) of that paper gives the frequency shift proportional to E as ($\vec{\omega}(t)$ lies in the x, y plane)

$$\delta\omega_E(t) = -\frac{1}{2}\int_0^t d\tau \left\{ \begin{array}{c} \cos\omega_o\tau\left[\vec{\omega}(t)\times\vec{\omega}(t-\tau)\right] \\ +\sin\omega_o\tau\left[\omega_x(t)\,\omega_x(t-\tau)+\omega_y(t-\tau)\,\omega_y(t)\right] \end{array} \right\} \tag{26}$$

It can be shown that the term multiplying $\sin\omega_o\tau$ goes to zero on averaging over a uniform velocity distribution $\left(\langle v_x v_y\rangle = 0, \quad v_x^2 = v_y^2 = v^2/2\right)$ and using $\overrightarrow{\nabla} \times \overrightarrow{B} = 0$.Then, for short times, τ,

$$\begin{aligned}\delta\omega(t) &= -\frac{1}{2}\int_0^t d\tau \left\{\cos\omega_o\tau \left[\overrightarrow{\omega}(t) \times \left(\overrightarrow{\omega}(t) - \frac{d\overrightarrow{\omega}}{dt}\tau + \frac{1}{2}\frac{d^2\overrightarrow{\omega}}{d\tau^2}\tau^2 + ...\right)\right]\right\} \\ &= -\frac{1}{2}\int_0^t d\tau \left\{\cos\omega_o\tau \left[-\overrightarrow{\omega}(t) \times \left(\frac{d\overrightarrow{\omega}}{dt}\tau - \frac{1}{2}\frac{d^2\overrightarrow{\omega}}{d\tau^2}\tau^2 + ...\right)\right]\right\} \qquad (27)\end{aligned}$$

We are considering values of τ so small that the velocity doesn't change in that time interval $(\tau < \tau_{coll})$.

Then

$$\begin{aligned}\overrightarrow{\omega}(t) &= \gamma\left(\overrightarrow{B}_{xy}(t) + \overrightarrow{v}/c \times \overrightarrow{E}\right) \\ \frac{d\overrightarrow{\omega}}{dt} &= \gamma\left(\overleftrightarrow{\nabla B}\left(\overrightarrow{x}(t)\right) \cdot \overrightarrow{v}\right) \\ \frac{d^2\overrightarrow{\omega}}{d\tau^2} &= \gamma\sum_{i,j}\frac{\partial^2\overrightarrow{B}}{\partial x_i \partial x_j}v_i v_j\end{aligned}$$

and

$$\delta\omega(t) = -\frac{\gamma}{2c}\int_0^t d\tau\cos\omega_o\tau\left[-\left(\overrightarrow{B}_{xy}(t) + \overrightarrow{v} \times \overrightarrow{E}\right) \times \left(\frac{\partial\overrightarrow{\omega}}{\partial t}\tau - \frac{1}{2}\frac{\partial^2\overrightarrow{\omega}}{\partial\tau^2}\tau^2 + ...\right)\right] \qquad (28)$$

The term linear in $\overrightarrow{E}$ and τ is then

$$\begin{aligned}\delta\omega(t) &= -\frac{\gamma^2}{2c}\int_0^t d\tau\cos\omega_o\tau\left[\left(\overleftrightarrow{\nabla B} \cdot \overrightarrow{v}\right)\tau \times \left(\overrightarrow{v} \times \overrightarrow{E}\right)\right] \\ &\equiv \frac{\gamma E}{2}\int_0^t d\tau\cos\omega_o\tau\,(\alpha\tau) \qquad (29)\end{aligned}$$

defining

$$\alpha = \frac{\gamma}{c}\left(\overleftrightarrow{\nabla B} \cdot \overrightarrow{v}\right) \cdot \overrightarrow{v}$$

We have now calculated the correlation function for short times. It starts at zero at $\tau = 0$ and rises as $\alpha\tau$. Eventually it will reach a maximum. By concentrating on the high frequency (ω_o) behavior of $\delta\omega$ the result will be independent of the details of the maximum, depending only on α. Thus we can replace $\alpha\tau$ in (29) by $\sin\alpha\tau$ or any function with the same initial slope. Thus we are led to take

$$\begin{aligned}\delta\omega(t) &\equiv \frac{\gamma E}{2}\lim_{\omega_o\to\infty}\int_0^t d\tau\cos\omega_o\tau\sin\alpha\tau \\ &= \lim_{\omega_o\to\infty}\frac{\gamma E}{2}\frac{\alpha}{\omega_o^2 - \alpha^2} = \frac{\gamma E}{2}\frac{\alpha}{\omega_o^2} \\ &= \frac{E}{2cB_o^2}\left(\overleftrightarrow{\nabla B} \cdot \overrightarrow{v}\right) \cdot \overrightarrow{v}\end{aligned}$$

Introducing components taking averages and using $\overrightarrow{\nabla} \cdot \overrightarrow{B} = 0$ this reduces to

$$\overline{\delta\omega}_{geo} = -Ev^2 \frac{1}{4cB_o^2} \left\langle \frac{\partial B_z}{\partial z} \right\rangle \tag{30}$$

in agreement with equ. (2) of [11] if, in that equation, $R^2\omega_r^2$ is replaced by $\langle v^2 \rangle = v^2/2$. We have shown that in the adiabatic (short time) limit the systematic (false) edm effect depends only on $\langle \frac{\partial B_z}{\partial z} \rangle$ regardless of the geometry of the magnetic field, a result obtained previously by Pendlebury et al [10] and confirmed in [17].

The next order term in (28) is easily seen to be of order $v^3\tau^2$ and so will average to zero, the next term which contributes will be of order $v^4\tau^3$ and so will be negligible in the short time limit we are considering. The condition for this to be valid is $(v\tau/\Lambda)^2 \ll 1$ where Λ is the scale of variations in the applied magnetic field $\left(\frac{\partial B_z}{\partial z} \frac{1}{B_z} \sim \Lambda^{-1} \right)$

5.2 Longer time behavior of the correlation function

For long times the expansion (27) is clearly not valid and we must expand in a series in the spatial coordinates. We start from

$$\delta\omega = -\frac{\gamma^2}{2} \int d\tau \cos\omega_o\tau \left\langle \overrightarrow{B}'(t) \times \overrightarrow{B}'(t-\tau) \right\rangle_z$$

where $b = E/c$, the brackets represent an ensemble average and

$$\begin{aligned} B_x' &= B_x(\overrightarrow{r}(t)) - bv_y \\ B_y' &= B_y(\overrightarrow{r}(t)) + bv_x \end{aligned}$$

Then we write

$$\left\langle \overrightarrow{B}'(t) \times \overrightarrow{B}'(t-\tau) \right\rangle_z = b \left\langle \begin{array}{c} B_x(\overrightarrow{r}(t))\, v_x(t-\tau) - v_y(t)\, B_y(\overrightarrow{r}(t-\tau)) \\ -\left(B_x(\overrightarrow{r}(t-\tau))\, v_x(t) - v_y(t-\tau)\, B_y(\overrightarrow{r}(t))\right) \end{array} \right\rangle \tag{31}$$

and expand the field in a Taylor series

$$\begin{aligned} B_x(\overrightarrow{r}(t)) = &\left(B_x(0,0,0,t) + \left.\frac{\partial B_x}{\partial x}\right|_o x(t) + \left.\frac{\partial B_x}{\partial y}\right|_o y(t) + \left.\frac{\partial B_x}{\partial z}\right|_o z(t) \right) + \\ &+ \left(\left.\frac{\partial^2 B_x}{\partial x^2}\right|_o x^2(t) + \left.\frac{\partial^2 B_x}{\partial y^2}\right|_o y^2(t) + \left.\frac{\partial^2 B_x}{\partial z^2}\right|_o z^2(t) \right) \\ &+ \left(\left.\frac{\partial^2 B_x}{\partial x \partial y}\right|_o y(t) x(t) + \left.\frac{\partial^2 B_x}{\partial y \partial z}\right|_o z(t)\, y(t) + \left.\frac{\partial^2 B_x}{\partial z \partial x}\right|_o x(t)\, z(t) \right) \\ &+ \left(\left.\frac{\partial^3 B_x}{\partial x^3}\right|_o x^3(t) + \left.\frac{\partial^3 B_x}{\partial y^3}\right|_o y^3(t) + ... \right) \end{aligned}$$

(similarly for B_y). Concentrating on the first and last terms in (31) and noting that there are no correlations between any functions $f(x_i, v_i)$ and $g(x_j, v_j)$ we find

$$\sum_{x_i=x,y} \left\langle \left(\left.\frac{\partial B_{x_i}}{\partial x_i}\right|_o x_i(t) + \left.\frac{\partial^2 B_{x_i}}{\partial x_i^2}\right|_o x_i^2(t) + \left.\frac{\partial^3 B_x}{\partial x_i^3}\right|_o x_i^3(t) \ldots \right) v_{x_i}(t-\tau) - \{(t) \Leftrightarrow (t-\tau)\} \right\rangle$$

where the second term is obtained from the first by interchanging (t) and $(t-\tau)$.

By symmetry we see that $\left\langle x_i^2(t)\, v_{x_i}(t-\tau) \right\rangle = 0$ so that the next contributing term will be proportional to

$$\left.\frac{\partial^3 B_x}{\partial x_i^3}\right|_o \left\langle x_i^3(t)\, v_{x_i}(t-\tau) \right\rangle$$

The first order term will be proportional to

$$\frac{\partial B_x}{\partial x} + \frac{\partial B_y}{\partial y} = -\frac{\partial B_z}{\partial z}$$

We see that the condition

$$\left.\frac{\partial^3 B_{x_i}}{\partial x_i^3}\right|_o R^2 \ll \left.\frac{\partial B_{x_i}}{\partial x_i}\right|_o \quad or \quad \frac{R^2}{\Lambda^2} \ll 1$$

will insure that the higher order terms can be neglected. In the extreme case considered by Harris and Pendlbury, [17], this condition is strongly violated so our method cannot be applied since the higher order terms remain significant.

6 Discussion

We see that in both the case of a velocity independent mean free path and one proportional to velocity the behavior of the systematic frequency shift is essentially unchanged. What is changed is the frequency where the effect goes to zero, i.e reduced frequency $\omega' \simeq 1.6$ in the case (1) of a constant mean free path and $\omega' \simeq 2$ for the case (2) of a mean free path proportional to velocity. This is because longer mean free paths contribute more to the frequency shift as seen from figure 1, and thus higher velocities contribute more to case (2). This shifts the effective frequency to higher values for the same value of reduced frequency.

Due to the heavy mass and slow velocity of the He^3, Baym and Ebner [18] conclude that the phonon scattering on He^3 is predominantly elastic. Single phonon absorption is kinematically forbidden on a single He^3 and can only take place as a result of $He^3 - He^3$ collisions which will be negligible for the low He^3 densities considered here. Thus our approach, where we calculate the correlation function for an ensemble of trajectories with constant He^3 velocity and then average the result over the velocity distribution should be an excellent approximation.

Note that for temperatures $T \gtrsim .38K, \quad r_o = 1/k \gtrsim 20$, so that according to fig.3 the limiting expression for the correlation function should be quite accurate and figures 10 and 11, which are based on an exact average over the Maxwell distribution of the He^3 velocities, imply that one should be able to control the effect to high degree.

What would be ideal, would be to set the size of the shift for He^3 to be slightly negative *i.e.* equal in sign and magnitude with the shift for UCN. The UCN, with their relatively low value of ω_r ($\omega_o/\omega_r \gg 1$), have a frequency shift which is represented by a point far to the right in figure 1).

The limits on the ability to do this will be the usual experimental ones of the temperature and magnetic field gradient stability.

We have shown that by varying the gradients to larger values it will be possible to measure the spectrum of the velocity correlation function directly, thus allowing a precise determination of the frequency dependence of the frequency shift under the exact experimental conditions.

References

[1] Weinberg, S. Proc. XXVI Inter. Conf. on High Energy Physics (Dallas, Texas) summary talk

[2] Pendlebury, JM and Hinds EA, NIM in Physics Research **A440**, 471 (2000)

[3] Golub, R and Lamoreaux, SK, Physics Reports, **237**, 1 (1994),

Harris, PG et al , PRL **82**, 904 (1999)

http://p25ext.lanl.gov/edm/edm.html

[4] Behr, JA et al, Eur. Phys. J. **A25**, 685 (2005)

[5] Berg, GPA et al, Nuclear Physics **A721**, 1107c (2003)

Schulte, E et al, 35th Meeting of the Division of Atomic, Molecular and Optical Physics, May 25-29, 2004, Tuscon AZ

Ahmad I et al, http://www-mep.phy.anl.gov/atta/research/radiumedm.html

Guest JR et al, Abstract KB.00011 2nd Joint Meeting of the Nuclear Physics Division of the APS and the Physical Society of Japan, Maui, Hawaii, Sept 18-22 (2005)

[6] Nuss-Warren et al, NIM in Physics Research **A533**, 275 (2004),

Abstrct KB.00010, 2nd Joint Meeting of the Nuclear Physics Division of the APS and the Physical Society of Japan, Maui, Hawaii, Sept 18-22 (2005)

[7] Rosenberry MA and Chupp TE, PRL **86**, 0031-9007 (2000)

Yoshimi A et al, Physics Letters, **A304**, 13 (2002) and

Abstract JB.00009, 2nd Joint Meeting of the Nuclear Physics Division of the APS and the Physical Society of Japan, Maui, Hawaii, Sept 18-22 (2005)

[8] Jacobs JP et al, Phys Rev **A52**, 3521 (1995)

[9] Commins, ED; Am. J. Phys. **59**, 1077 (1991)

[10] Pendlebury, JM *et al;* Phys. Rev. **A70**, 032102 (2004)

[11] Lamoreaux, SK and Golub, R; Phys. Rev **A71**, 032104 (2005)

[12] http://p25ext.lanl.gov/edm/edm.html

[13] Lamoreaux, SK *et al*; Europhys Lett. **58**, 718 (2002)

[14] McGregor, DD, Phys Rev **A41**, 2631 (1990)

[15] Abramowitz, M. and Stegun, IA, *Handbook of mathematical functions*, NBS, (1964)

[16] Papoulis, A, *Probability, Random Variables and Stochastic Processes,* McGraw Hill, NY (1965)

[17] Harris, PG and Pendlebury, JM, *"Dipole field contributions to geometric phase induces false electric dipole moment signals for particles in traps"*, arxiv.org: physics/0510134, ct. 2005

[18] Baym, G and Ebner, C; Phys. Rev. **164**, 235 (1967)

7 Figure Captions

Figure 1. Note the curves are for a single fixed velocity. The velocity dependence is contained in the normalization of the frequency scale, $\omega_r = v/R$.

Figure 2. Trajectory of a particle confined in a cylindrical vessel.

Figure 3a. Comparison of correlation function, $R(\tau)$ from numerical simulations and from the analytic model. red - numerical simulation, blue - complete model equation (11), green - short mean free path limit equation (14) where appropriate. $r_o = R/\lambda = 50, 10$.

Figure 3b) As figure 3a) $r_o = 0.5, 1, 2.5, 6, 7.5$
Figure 3c. Dependence of $k = \lambda(T)/R$ on temperature.

Figure 4. Normalized, velocity averaged fequency shift vs. normalized frequency: $X(\omega, T) = \omega R/\beta(T)$. red T=0.3K, blue 0.35K, green 0.4K, purple 0,45K

Figure 5. Normalized, velocity averaged fequency shift vs. normalized frequency, expanded scale. red T=0.3K, blue 0.35K, green 0.4K, purple 0,45K

Figure 6. Normalized, velocity averaged fequency shift vs. normalized frequency. Same as figure 8, but expanded further. red T=0.3K, blue 0.35K, green 0.4K, purple 0,45K

Figure 7. Velocity averaged frequency shift as a function of temperature, K, for various frequencies., red X=1.4, blue X=1.5, green X=1.7, purple X=1.8

Figure 8. Velocity averaged frequency shift as a function of temperature, K, for various frequencies. As figure 7, scale expanded to show experimetnally interesting region, red X=1.4, blue X=1.5, green X=1.6, purple X=1.7, light blue X=1.8

Figure 9. Frequency shift averaged over velocity distribution, allowing for velocity dependence of the He^3 mean free path, for various temperatures. X is the normalized frequency, $X = \omega R/\beta(T)$ with $\beta(T)$ the most probable He^3 velocity. green T=0.35K, purple T=0.38K, red T=0.4K, blue T=0.43K.

Figure 10. Frequency shift averaged over velocity distribution, allowing for velocity dependence of the He^3 mean free path, versus temperature, K, for various frequencies specified by the value of $X = \omega R/\beta$ with β the most probable He^3 velocity. blue X=3, green X=2.2, red X=2, purple X=1.8.

Figure 11. Expanded plot of the frequency shift averaged over velocity distribution, allowing for velocity dependence of the He^3 mean free path, versus temperature, K, for various frequencies specified by the value of $X = \omega R/\beta(T)$ with $\beta(T)$ the most probable He^3 velocity. blue X=3, green X=2.2, red X=2, purple X=1.8.

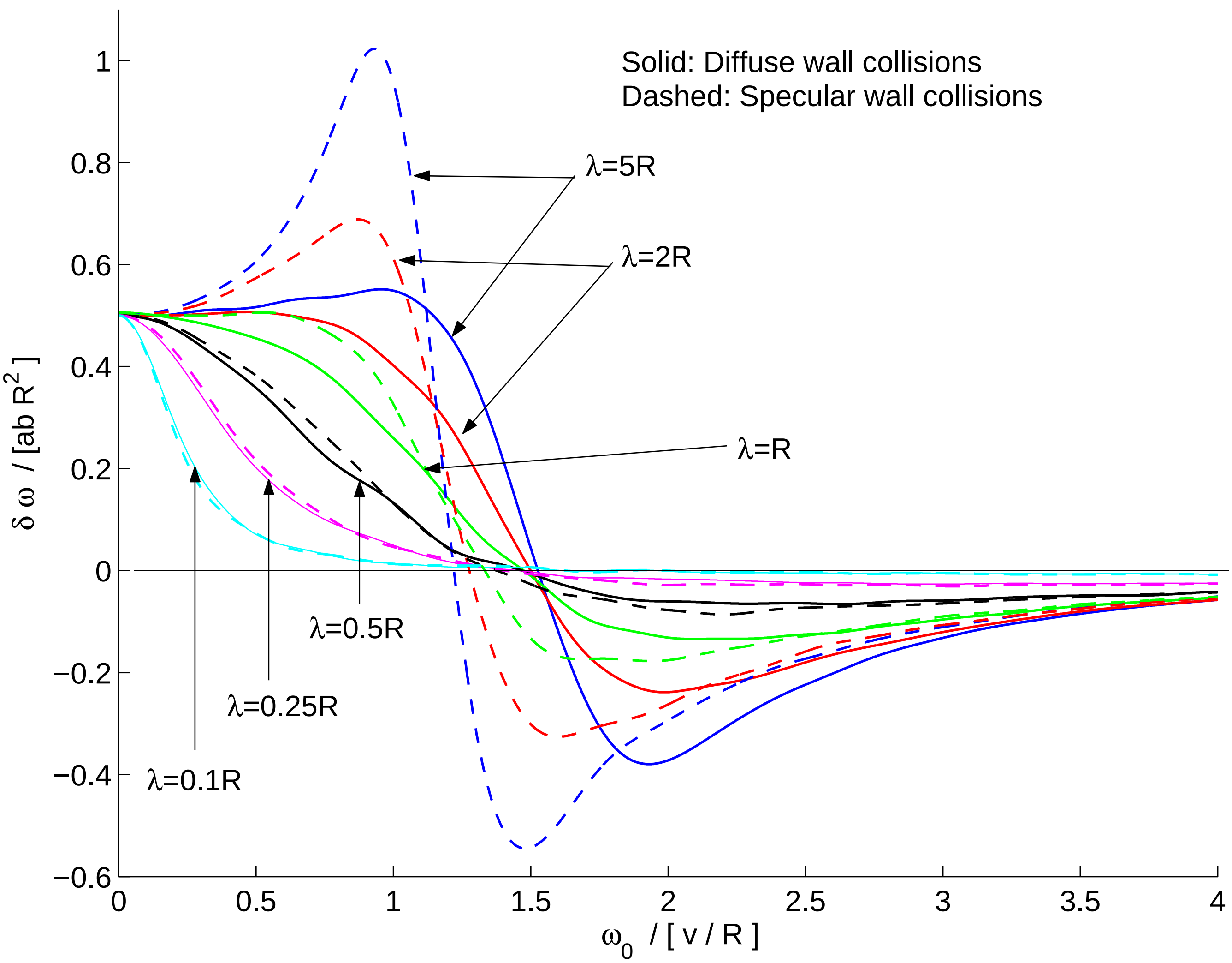
Solid: Diffuse wall collisions
Dashed: Specular wall collisions
λ=5R
λ=2R
λ=R
λ=0.5R
λ=0.25R
λ=0.1R
δ ω / [ab R^2]
ω_0 / [v / R]
1
0.8
0.6
0.4
0.2
0
−0.2
−0.4
−0.6
0
0.5
1
1.5
2
2.5
3
3.5
4

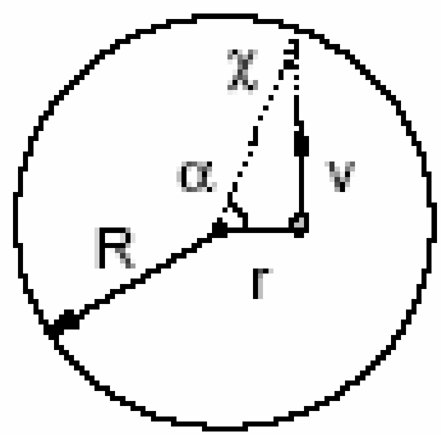
χ
α
v
R
r

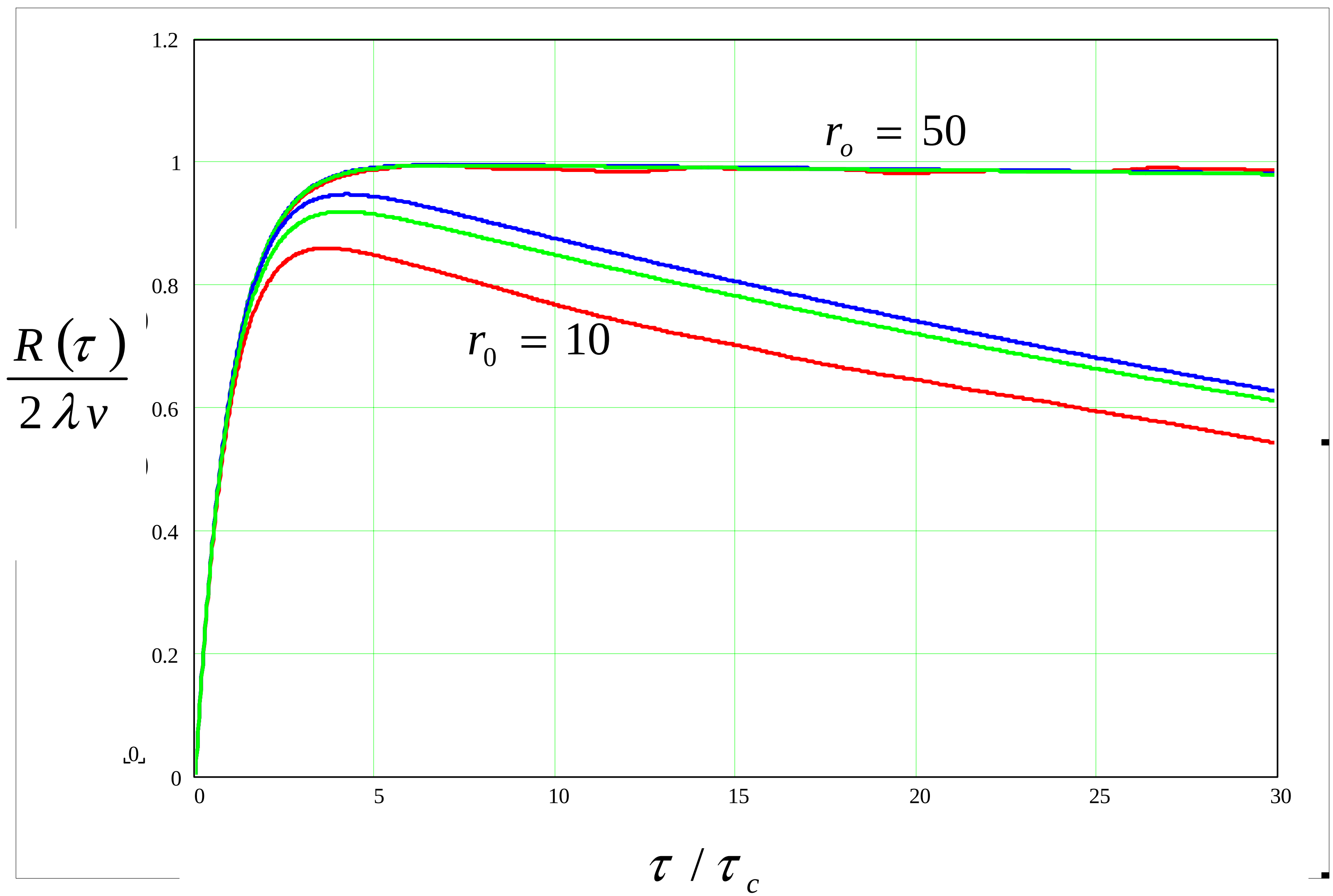

1.2
1
0.8
0.6
0.4
0.2
0
$\frac{R(\tau)}{2\lambda v}$
$r_o = 50$
$r_0 = 10$
0
5
10
15
20
25
30
τ / τ_c

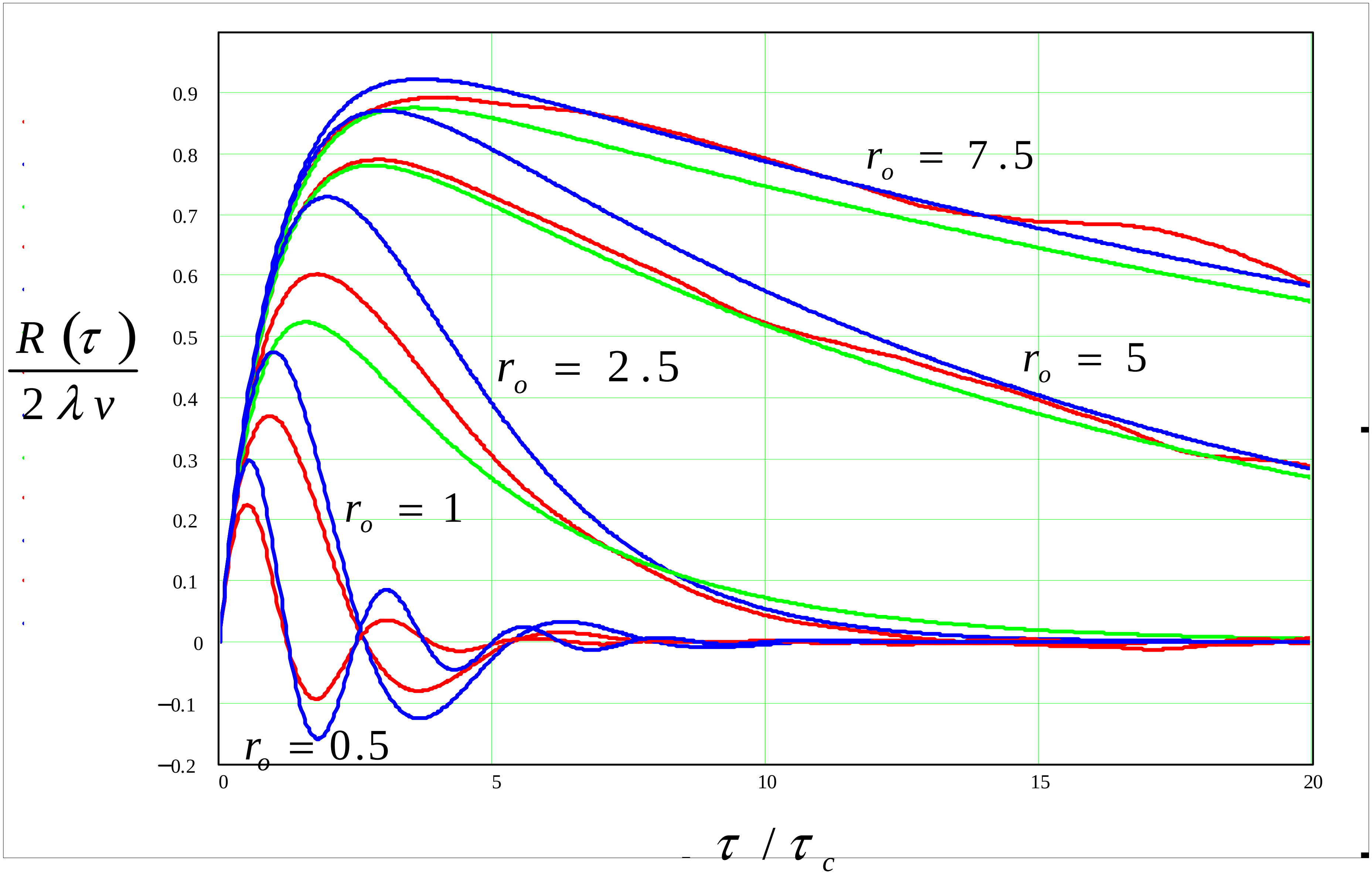

R(τ) / 2λν
0.9
0.8
0.7
0.6
0.5
0.4
0.3
0.2
0.1
0
−0.1
−0.2
0
5
10
15
20
τ / τc
ro = 7.5
ro = 5
ro = 2.5
ro = 1
ro = 0.5

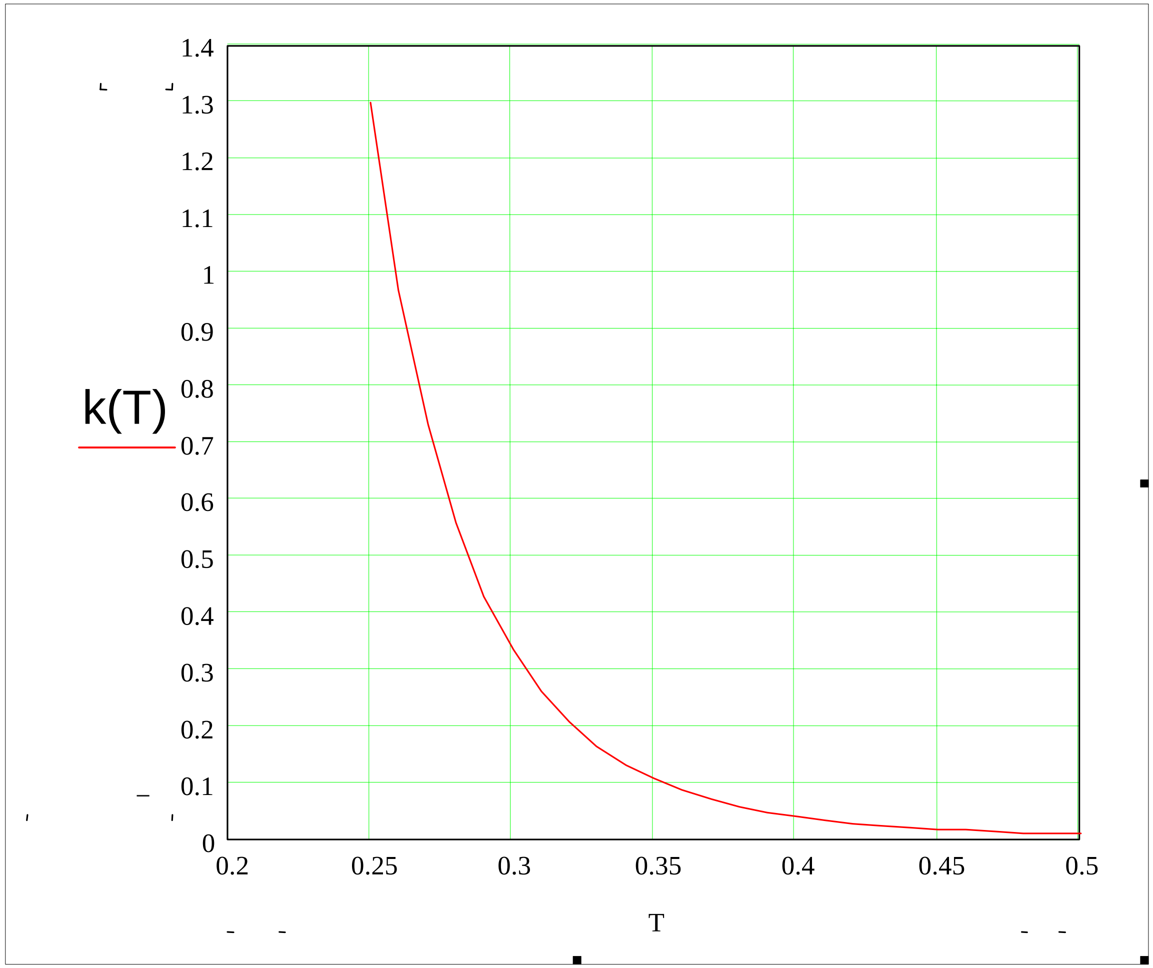

k(T)
1.4
1.3
1.2
1.1
1
0.9
0.8
0.7
0.6
0.5
0.4
0.3
0.2
0.1
0
0.2
0.25
0.3
0.35
0.4
0.45
0.5
T

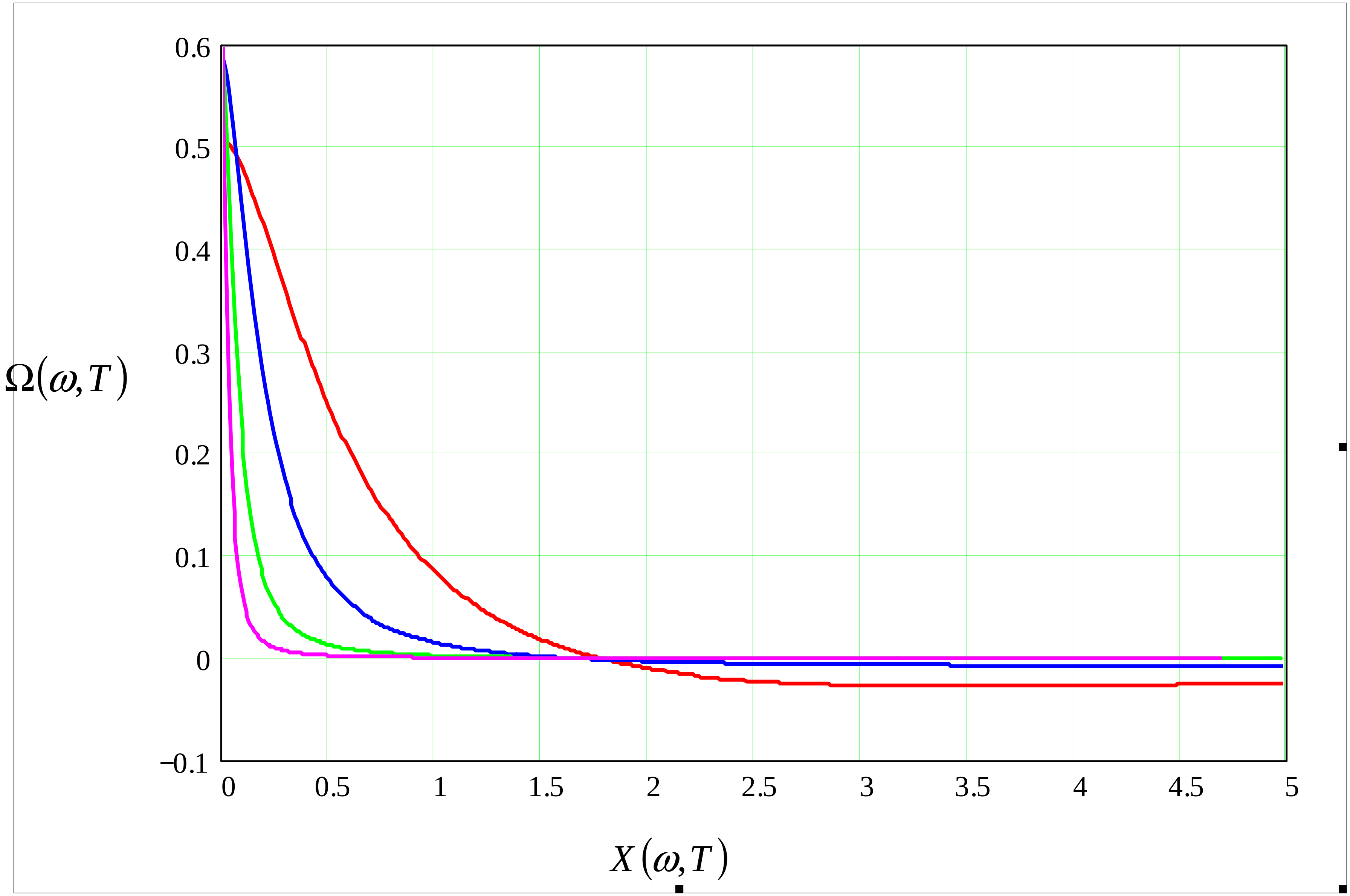

0.6
0.5
0.4
0.3
0.2
0.1
0
−0.1
Ω(ω,T)
0
0.5
1
1.5
2
2.5
3
3.5
4
4.5
5
X(ω,T)

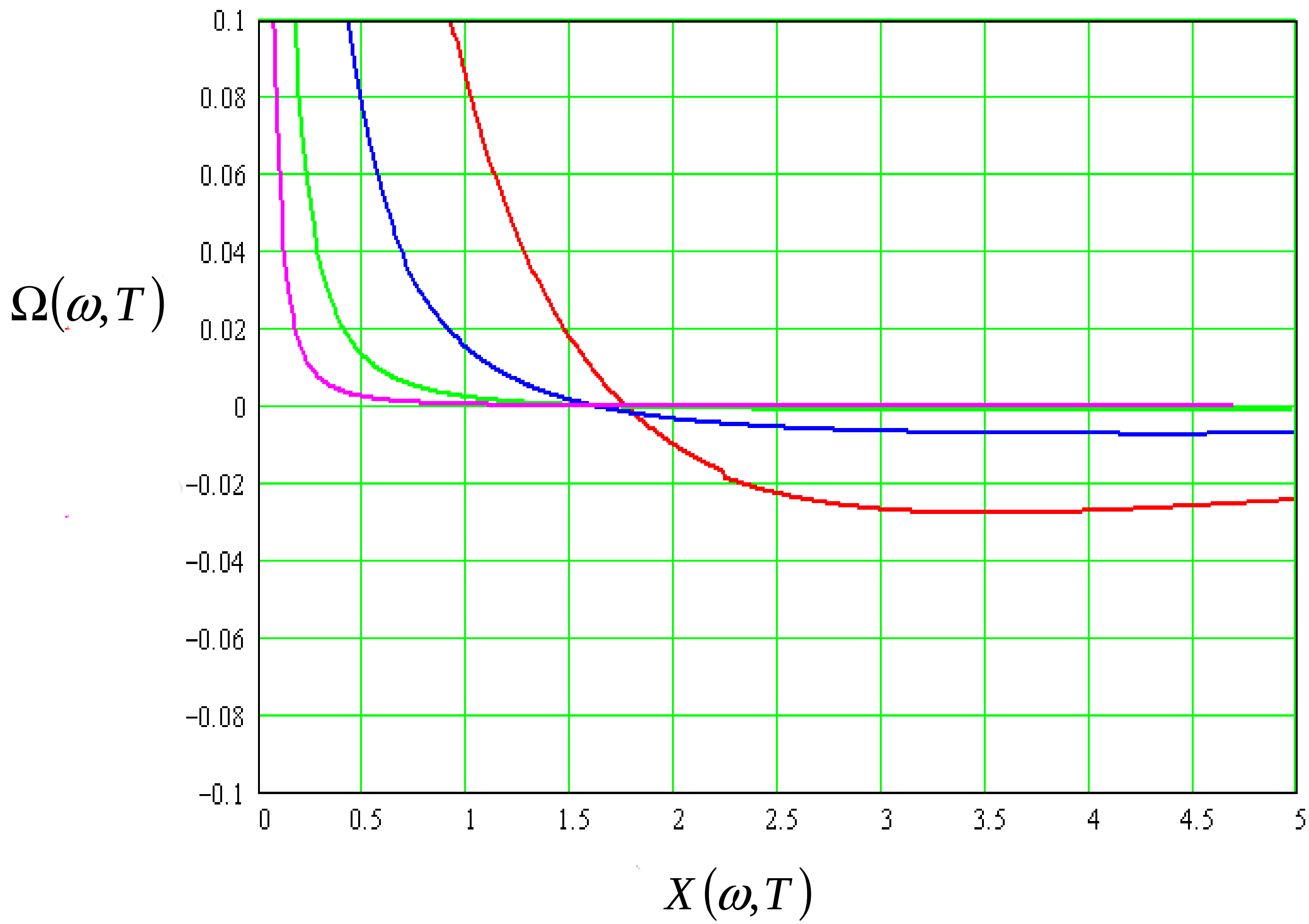

Ω(ω,T)
0.1
0.08
0.06
0.04
0.02
0
−0.02
−0.04
−0.06
−0.08
−0.1
0
0.5
1
1.5
2
2.5
3
3.5
4
4.5
5
X(ω,T)

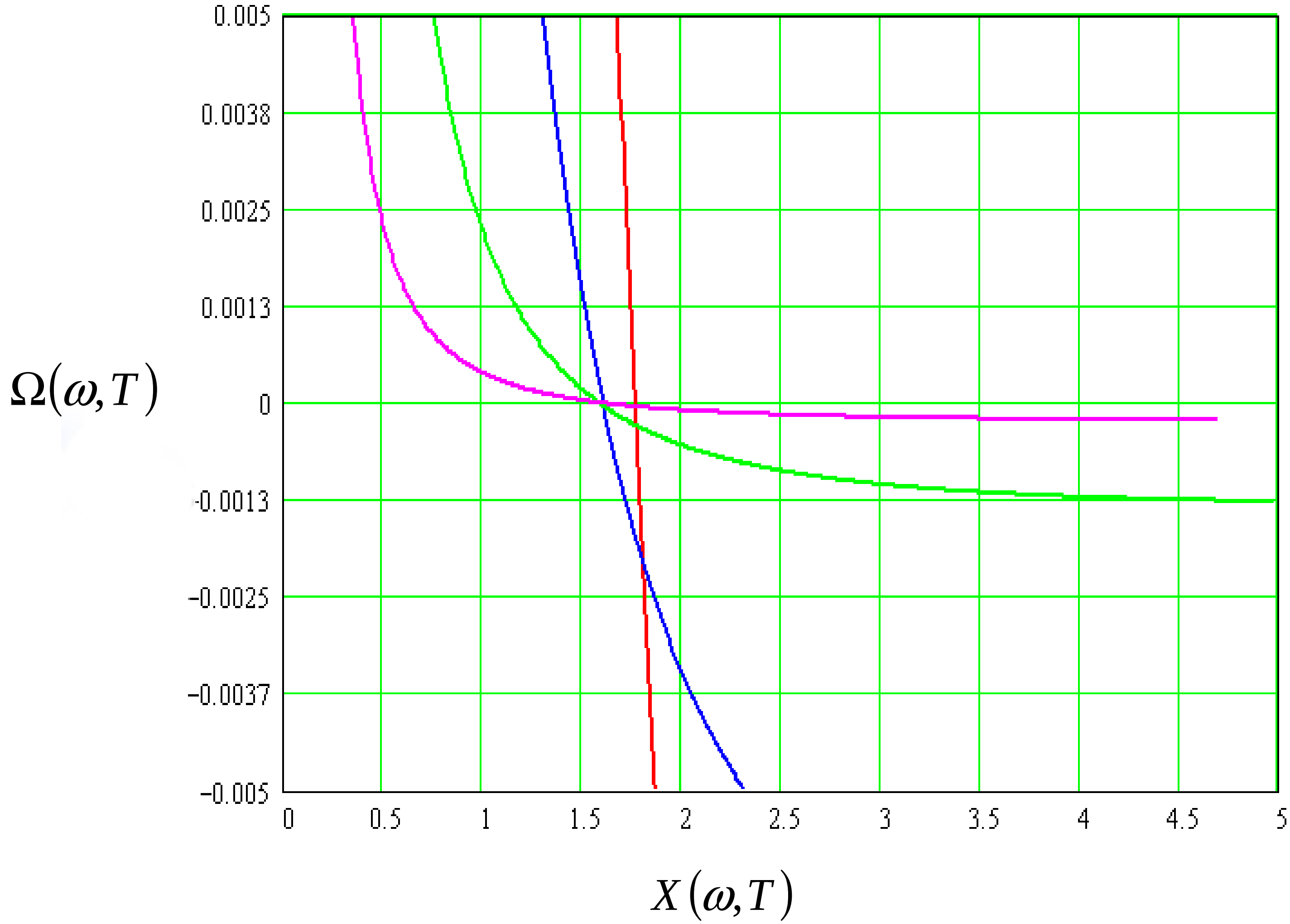

0.005
0.0038
0.0025
0.0013
0
-0.0013
−0.0025
−0.0037
−0.005
0
0.5
1
1.5
2
2.5
3
3.5
4
4.5
5
Ω(ω,T)
X(ω,T)

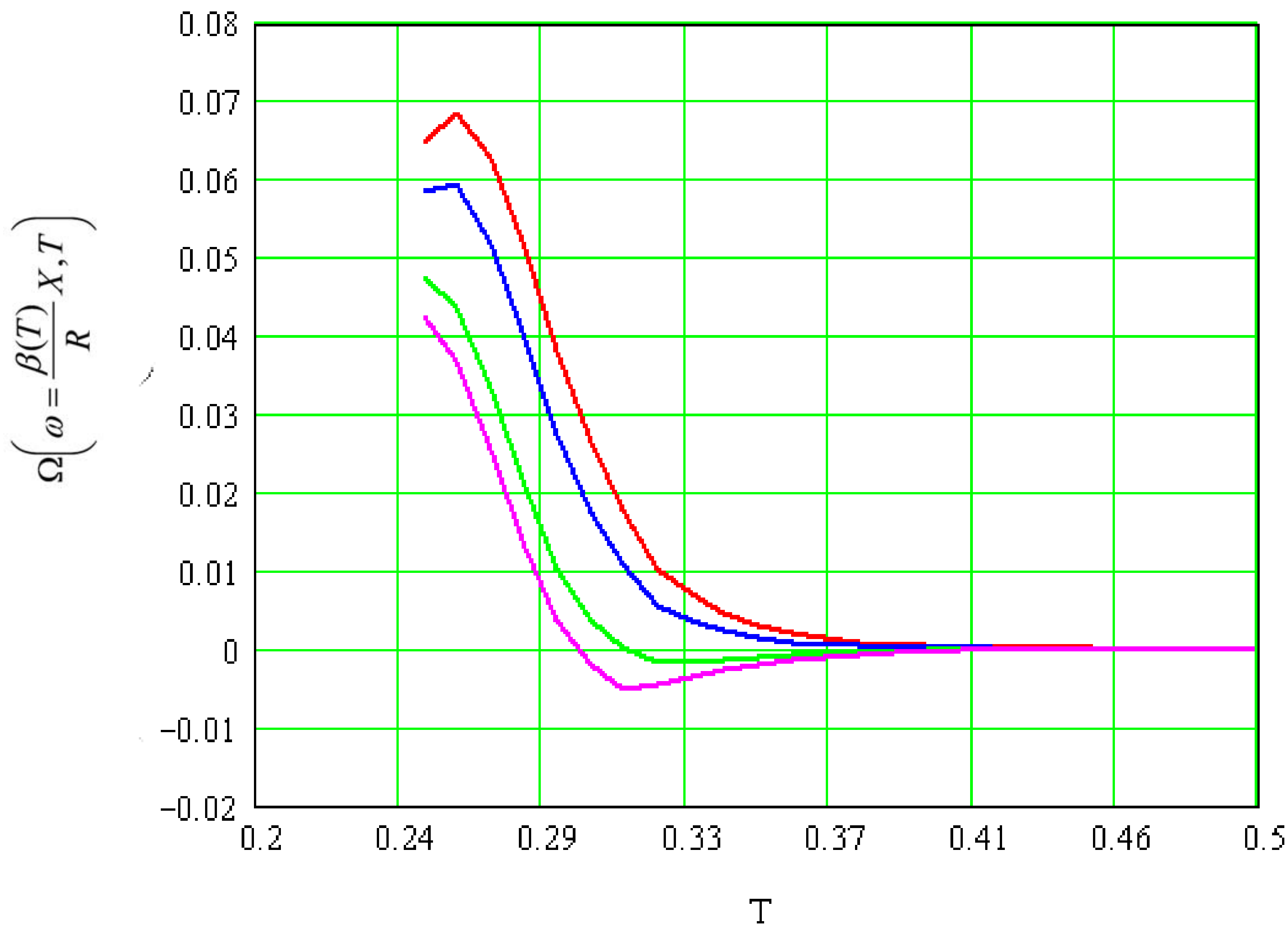

0.08
0.07
0.06
0.05
0.04
0.03
0.02
0.01
0
−0.01
−0.02
0.2
0.24
0.29
0.33
0.37
0.41
0.46
0.5
$\Omega\left(\omega = \frac{\beta(T)}{R} X, T\right)$
T

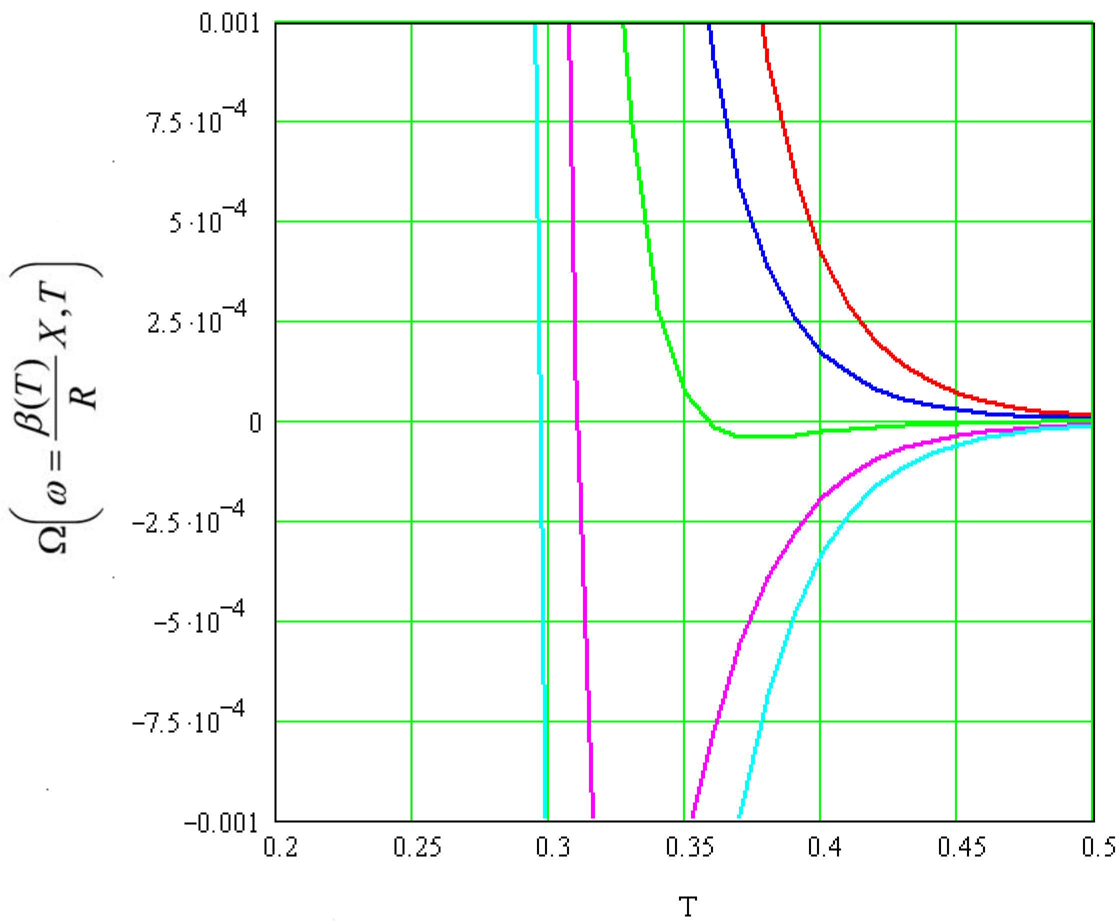

$\Omega\left(\omega = \frac{\beta(T)}{R} X, T\right)$
0.001
$7.5 \cdot 10^{-4}$
$5 \cdot 10^{-4}$
$2.5 \cdot 10^{-4}$
0
$-2.5 \cdot 10^{-4}$
$-5 \cdot 10^{-4}$
$-7.5 \cdot 10^{-4}$
−0.001
0.2
0.25
0.3
0.35
0.4
0.45
0.5
T

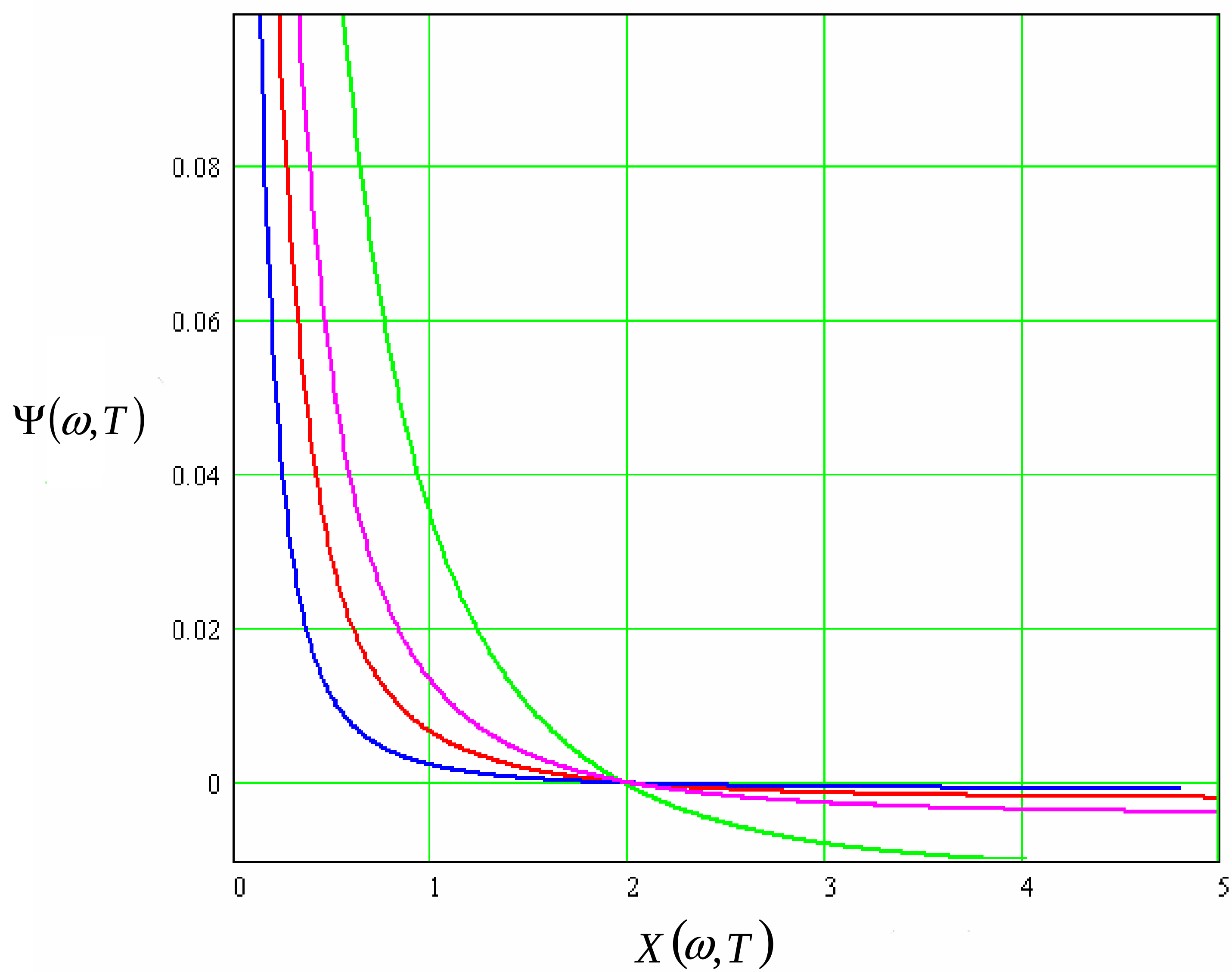
0.08
0.06
0.04
0.02
0
Ψ(ω,T)
0
1
2
3
4
5
X(ω,T)

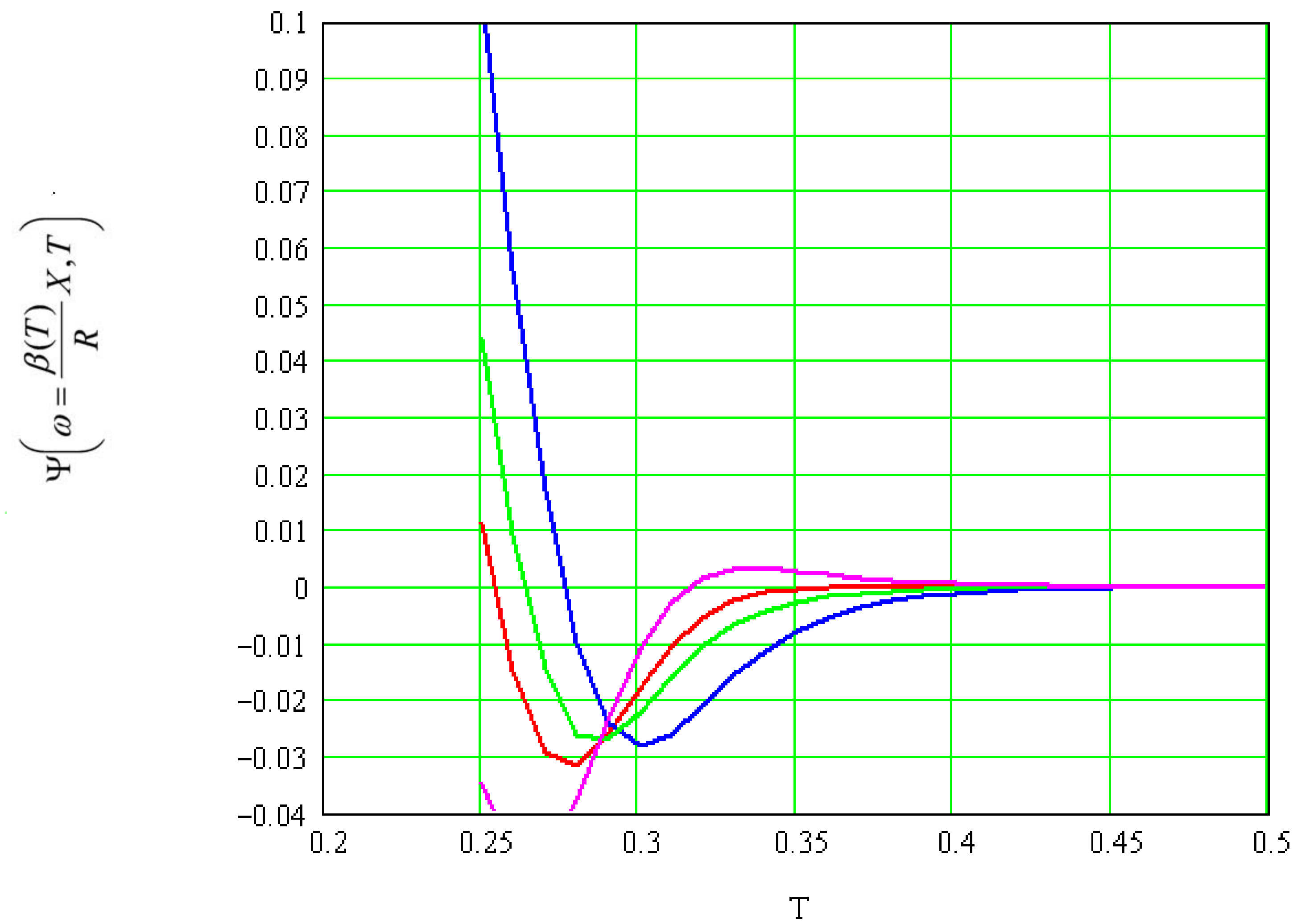
$\Psi\left(\omega = \frac{\beta(T)}{R} X, T\right)$
0.1
0.09
0.08
0.07
0.06
0.05
0.04
0.03
0.02
0.01
0
−0.01
−0.02
−0.03
−0.04
0.2
0.25
0.3
0.35
0.4
0.45
0.5
T

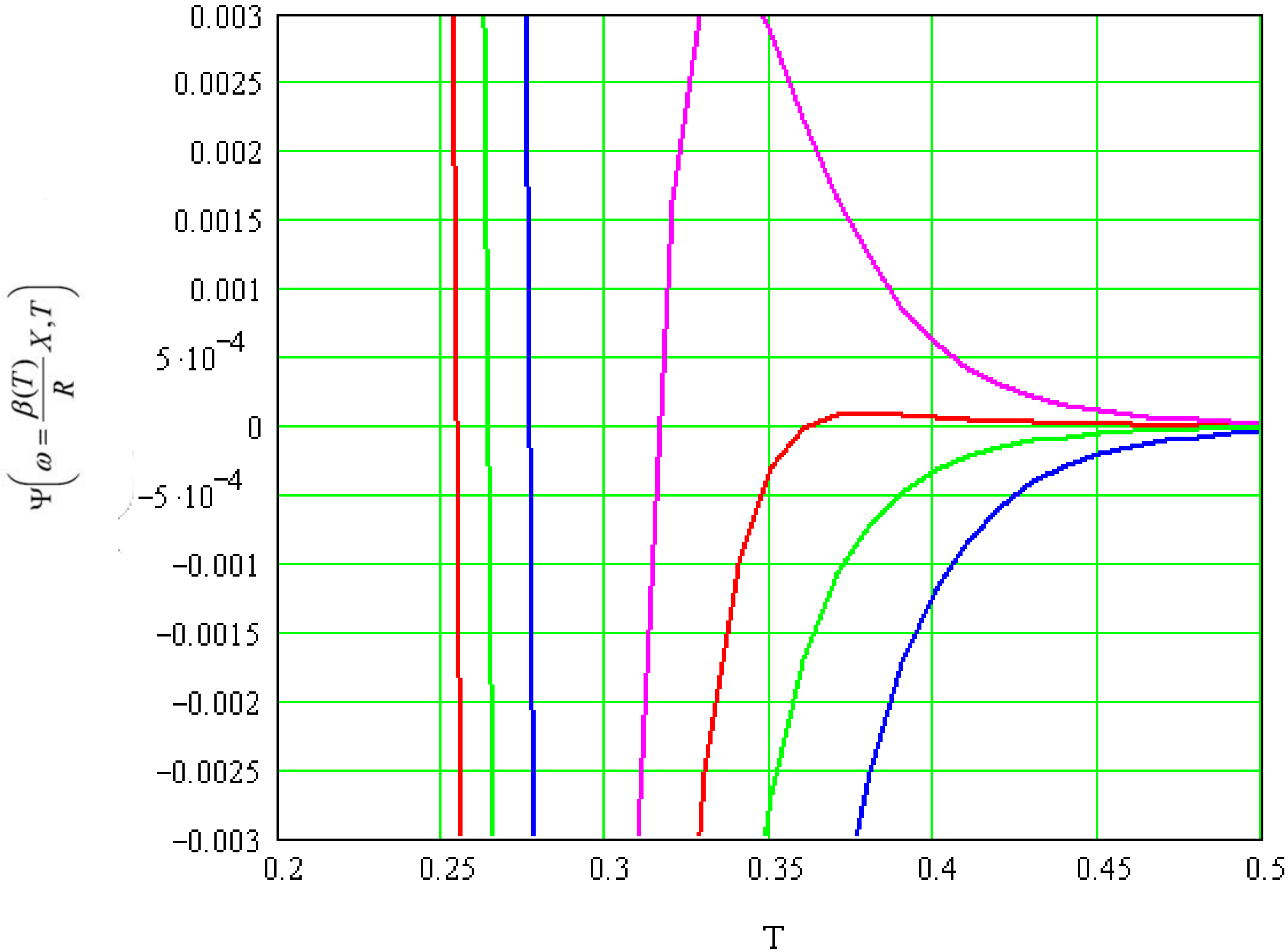
0.003
0.0025
0.002
0.0015
0.001
$5 \cdot 10^{-4}$
0
$-5 \cdot 10^{-4}$
−0.001
−0.0015
−0.002
−0.0025
−0.003
0.2
0.25
0.3
0.35
0.4
0.45
0.5
T
$\Psi\left(\omega = \frac{\beta(T)}{R} X, T\right)$